Article ID: 1000-324X(2021)10-1118-07 **DOI:** 10.15541/jim20210059

Fine-grained Ce,Y:$SrHfO_3$ Scintillation Ceramics Fabricated by Hot Isostatic Pressing

ZHU Danyang[1,2], QIAN Kang[1,3], CHEN Xiaopu[1,2], HU Zewang[1,2], LIU Xin[1,2], LI Xiaoying[1,2], PAN Yubai[3], MIHÓKOVÁ Eva[4], NIKL Martin[4], LI Jiang[1,2]

(1. Key Laboratory of Transparent Opto-functional Inorganic Materials, Shanghai Institute of Ceramics, Chinese Academy of Sciences, Shanghai 201899, China; 2. Center of Materials Science and Optoelectronic Engineering, University of Chinese Academy of Sciences, Beijing 100049, China; 3. Department of Physics, Shanghai Normal University, Shanghai 200234, China, 4. Institute of Physics, Academy of Sciences of the Czech Republic, Prague 16200, Czech Republic)

Abstract: Ce:$SrHfO_3$ ceramics possess a strong stopping power to high-energy rays due to their high density and high effective atomic number. However, it is difficult to obtain transparent Ce:$SrHfO_3$ ceramics *via* traditional sintering method because of its orthogonal structure. In this work, Ce,Y:$SrHfO_3$ ceramics were prepared by long-time vacuum sintering and short-time vacuum pre-sintering combined with hot isostatic pressing (HIP). The Ce,Y:$SrHfO_3$ powders with a pure phase and a mean particle size of 152 nm were prepared by calcining at 1200 ℃ for 8 h using metal oxides and carbonates. The Ce,Y:$SrHfO_3$ ceramics vacuum-sintered at 1800 ℃ for 20 h are opaque with an average grain size of 28.6 μm, while those prepared by the two-step sintering method show good optical transmittance. The evolution of the microstructure in the process of densification was analyzed in detail, and the influence of the pre-sintering temperature on the density, microstructure and optical transparency of Ce,Y:$SrHfO_3$ ceramics was studied. The Ce,Y:$SrHfO_3$ ceramics pre-sintered at 1500 ℃ for 2 h with HIP post-treatment at 1800 ℃ for 3 h have the highest in-line transmittance of 21.6% at 800 nm with a far smaller average grain size of 3.4 μm. Under X-ray excitation, the Ce^{3+} 5d-4f emission of Ce,Y:$SrHfO_3$ ceramics was observed at 400 nm, and the XEL integral intensity is 3.3 times higher than that of $Bi_4Ce_3O_{12}$ (BGO) crystals. The light yield of the Ce,Y:$SrHfO_3$ ceramics is approximately 3700 ph/MeV with the shaping time of 1 μs. Good optical quality and scintillation performance of Ce,Y:$SrHfO_3$ ceramics may expand the application range and potential in the field of scintillation detection.

Key words: Ce,Y:$SrHfO_3$ ceramics; hot isostatic pressing; microstructure; grain refinement; scintillation properties

Scintillation materials are widely used in high energy physics, nuclear medicine imaging, security techniques and other X/γ ray or particle beam detection devices[1-4]. The requirements on the scintillation material performance differ in various fields, but high density, high effective atomic number, high light yield, fast scintillation decay, good time and energy resolution are generally required[5-8]. In recent years, new types of hafnate scintillators[9-18] have attracted wide attention, especially $SrHfO_3$[19-25]. However, $SrHfO_3$ is difficult to prepare in the single crystal form because of its high melting point over 2700 ℃. It was reported[26] that Ce doped $SrHfO_3/SrAl_{12}O_{19}$ eutectics were prepared by the micro pulling down (μ-PD) method. Nevertheless, the size of eutectic is too small to provide practical application value. Fortunately, optical ceramic technology has gained great progress. Compared to single crystals, transparent ceramics could be obtained under suitable fabrication

Received date: 2021-02-01; **Revised date:** 2021-03-29; **Published online:** 2021-05-10
Foundation item: National Key R&D Program of China (2017YFB0310500); National Natural Science Foundation of China (61775226); CAS President's International Fellowship Initiative (E00YGH21); Operational Programme Research, Development and Education financed by European Structural and Investment Funds and the Czech Ministry of Education, Youth and Sports (SOLID21 CZ.02.1.01/0.0/0.0/16_019/0000760)
Biography: ZHU Danyang (1997–), female, PhD candidate. E-mail: zhudanyang@student.sic.ac.cn
朱丹阳(1997–), 女, 博士研究生. E-mail: zhudanyang@student.sic.ac.cn
Corresponding author: LI Jiang, professor. E-mail: lijiang@mail.sic.ac.cn
李 江, 研究员. E-mail: lijiang@mail.sic.ac.cn

conditions with larger size, lower cost and more flexible composition design[27-30]. Likewise, it is relatively easy to prepare hafnate ceramics at lower temperatures. Ce:$SrHfO_3$ ceramics have a high density (7.56 g/cm^3) and effective atomic number (64), both providing rather high radiation stopping power. Ce:$SrHfO_3$ ceramics show fast scintillation decay (21.6–42 ns) due to fast 5d-4f radiative transition of Ce^{3+}. Excellent timing resolution (276 ps) of Ce:$SrHfO_3$ ceramics is comparable to that of commercial high-quality LSO:Ce,Ca crystals[31]. However, the structure of $SrHfO_3$ is orthorhombic (Pnma) at room temperature, and the birefringence effect caused by its non-cubic phase structure makes the polycrystalline ceramics difficult to be transparent. Moreover, there is a series of phase transitions during the sintering process[32]. The frequent change of the cell size hinders the densification of the ceramics. Pressure sintering (hot isostatic pressing or hot pressing) is an effective method to promote the densification of ceramics. Ce:$SrHfO_3$ ceramics have been successfully prepared by vacuum hot pressing[22,31]. Since the graphite dies used in vacuum hot pressing causes inevitable carbon pollution, hot isostatic pressing (HIP) might prove advantageous. Hot isostatic pressing is a sintering process in which materials are subjected to balanced pressure in all directions to receive higher driving force so that the ceramics could be fully dense at lower sintering temperature with shorter time[33].

There are many factors affecting scintillation property of materials. Structural design and scintillation property of materials are sometimes shaped by co-doping. When Ce^{3+} substitutes Sr^{2+} in the Ce:$SrHfO_3$ ceramics, the charge imbalance causes the production of Ce^{4+} and interstitial oxygen, which leads to deterioration of scintillation property. By aluminum co-doping, Al^{3+} substitutes for Hf^{4+} and the effective charge compensation increases the Ce^{3+}/Ce^{4+} ratio[34], which improves the optical and scintillation performance. It has also been proved in our previous work[35]. As another common trivalent co-dopant, yttrium is supposed to have similar effect in the charge compensation as aluminum. Moreover, adding yttrium oxide is also expected to be beneficial to the densification process of the Ce:$SrHfO_3$ ceramics, which could lead to better optical performance.

In this work, Ce,Y:$SrHfO_3$ powders were prepared by solid-state synthesis. Ce,Y:$SrHfO_3$ ceramics were successfully fabricated by vacuum pre-sintering combined with hot isostatic pressing (HIP). The influence of calcination temperature on the phase composition, particle size and morphology of the powders was systematically investigated. In addition, the crystal structure, luminescence, and scintillation property of Ce,Y:$SrHfO_3$ ceramics were also investigated.

1 Experimental

The $Ce_{0.005}$,$Y_{0.005}$:$Sr_{0.995}Hf_{0.995}O_3$ powders were prepared by solid-state reaction. Commercial powders of HfO_2 (99.99%), $SrCO_3$ (99.95%), CeO_2 (99.99%), and Y_2O_3 (99.99%) were used as starting materials. These powders were weighed according to the formula of $Ce_{0.005}$,$Y_{0.005}$:$Sr_{0.995}Hf_{0.995}O_3$ following a mixing and ball-milling process for 12 h in ethanol solvent at a rotation speed of 130 r/min. The obtained slurries were dried and sieved. Then the mixed powders were calcined in alumina crucibles at different temperatures for 8 h to obtain $Ce_{0.005}$,$Y_{0.005}$:$Sr_{0.995}Hf_{0.995}O_3$ powders. Mixed powders were pressed into discs and cold isostatically pressed under 250 MPa. A part of the $Ce_{0.005}$,$Y_{0.005}$:$Sr_{0.995}Hf_{0.995}O_3$ discs were further vacuum-sintered at 1850 ℃ for 20 h. The other part of discs were pre-sintered at 1450–1650 ℃ for 2 h in a vacuum furnace (10^{-5} Pa) and subsequently hot isostatically pressed at 1800 ℃ in Ar and under the pressure of 200 MPa for 3 h. Finally, all $Ce_{0.005}$,$Y_{0.005}$:$Sr_{0.995}Hf_{0.995}O_3$ ceramics were double mirror-polished to the thickness of 1 mm for following characterization. In order to get sharp microstructure pictures of grain boundaries, a thermal etching process was applied before SEM, in which the ceramic sample was kept at 1400 ℃ for 3 h in air.

The structural phase of the calcined powders was identified by the X-ray diffraction (XRD, Cu-Kα radiation 0.154 nm Mode-l D/max2200PC, Rigaku, Japan). The microstructure and morphology of powders were observed by field emission scanning electron microscope (FESEM, S-4800, Hitachi, Japan). Morphology of the ceramics was observed by field emission scanning electron microscope (FESEM, SU8220, Hitachi, Japan). The specific surface area analysis was conducted by Norcross ASAP 2010 micromeritics, using N_2 as an absorbate gas at 77 K. The density of ceramics was measured by the Archimedes method using deionized water as the immersion medium. The X-ray excited luminescence (XEL) measurements were conducted by a home-made X-ray excited luminescence spectrometer. The excitation F30III-2 X-ray tube was operated at 70 kV with a tungsten target. Light yield measurement was accomplished by the measurement of pulse height spectra under the 662 keV γ-ray excitation (^{137}Cs source) and detection by a Hamamatsu R878 photomultiplier with 1 μs shaping time.

2 Results and discussion

Fig. 1(a-f) shows the FESEM micrographs of four types of raw material powders, the ball-milled powder mixture and the powder calcined at 1200 ℃ for 8 h. It can be seen from Fig. 1(a, b) that the HfO_2 and $SrCO_3$ powders consist of nearly spherical particles with the uniform shape and particle size. The CeO_2 and Y_2O_3 powders have the block structure with the particle size larger than 1 μm as shown in Fig. 1(c, d). After the ball milling, the powders with large particle size are effectively broken into small particles, and different powders are well dispersed and uniformly mixed as shown in Fig. 1(e). After being calcined at 1200 ℃ for 8 h in air, Ce,Y:$SrHfO_3$ powder is slightly agglomerated and of fairly uniform size, with an average particle size of approximate 152 nm as shown in Fig. 1(f), which possesses a strong sintering activity. Compared with the standard XRD pattern of orthorhombic $SrHfO_3$ (PDF#45- 0212), the Ce,Y:$SrHfO_3$ powders consist of the $SrHfO_3$ phase without other intermediate phases detected, as shown in Fig. 1(g). The diffraction peaks of the calcined powders slightly move to the high angle, which is caused by the fact that smaller trivalent cerium ions enter the lattice to replace the position of the bivalent strontium ions. First, to fabricate fully dense ceramic, a long-time vacuum sintering was implemented. As shown in Fig. 1(h), the Ce,Y:$SrHfO_3$ ceramics sintered at 1800 ℃ for 20 h in vacuum appear opaque. The average grain size of Ce,Y:$SrHfO_3$ ceramics was measured to be about 28.6 μm. The large grains arranged in disorder cause severe birefringent effect in asymmetric system and reduce the optical transmittance of the ceramics. Except for the large grain size, a large number of intracrystalline and intergranular pores are observed in Ce,Y:$SrHfO_3$ ceramics. It is well known that the pores in the microstructures of transparent ceramics are the primary light scattering sources. In order to further improve the optical quality of ceramics, an alternative way of preparation consisting in the low-temperature vacuum pre-sintering and HIP post-treatment was used, which was expected to eliminate residual pores while maintaining fine grains.

Fig. 2(a-e) shows the FESEM microstructures of the thermally etched surfaces of the Ce,Y:$SrHfO_3$ ceramics pre-sintered at different temperatures for 2 h. It can be seen that the grain boundaries of Ce,Y:$SrHfO_3$ ceramics pre-sintered at different temperatures are clearly visible, and neither impurities nor the second phase appears at the grain boundaries. With the increase of pre-sintering temperature, the small pores between grains gathered

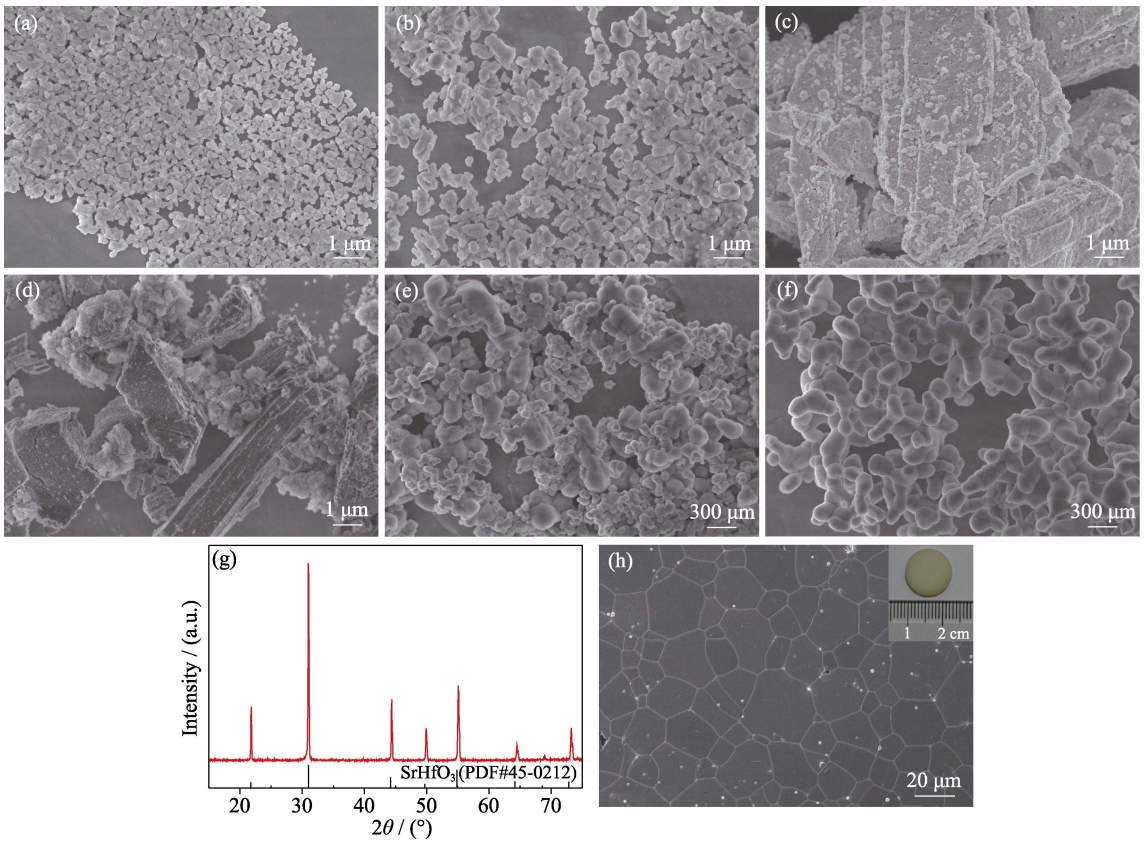

Fig. 1 FESEM micrographs of the starting powders ((a) HfO_2, (b) $SrCO_3$, (c) CeO_2, (d) Y_2O_3, (e) ball-milled powder mixture, (f) Ce,Y:$SrHfO_3$ powder calcined at 1200 ℃ for 8 h), (g) XRD patterns of the calcined powder, and (h) FESEM micrograph of the Ce,Y:$SrHfO_3$ ceramics fabricated by vacuum sintering

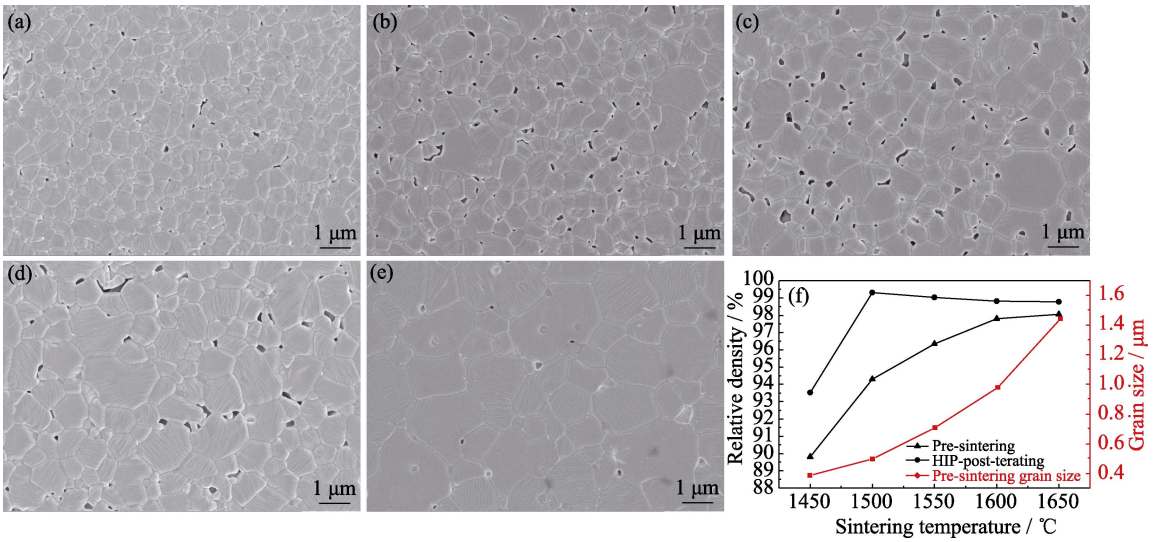

Fig. 2　FESEM images of the thermally etched surfaces of the Ce/Y:$SrHfO_3$ ceramics pre-sintered at different temperatures for 2 h (a) 1450 ℃; (b) 1500 ℃; (c) 1550 ℃; (d) 1600 ℃; (e) 1650 ℃; (f) Relative densities and average grain sizes of the Ce,Y:$SrHfO_3$ ceramics with different pre-sintering temperatures

into bigger ones and were then gradually eliminated. The grain size becomes larger, and the ceramics become more compact. When the pre-sintering temperature reaches 1650 ℃, the ceramics are basically compact but some intracrystalline pores appear at this temperature. The relative densities of the Ce,Y:$SrHfO_3$ ceramics before and after HIP post-treatment at different pre-sintering temperatures and the average grain size of the pre-sintered body calculated from the FESEM microstructures are shown in Fig. 2(f). With the sintering temperature increasing from 1450 to 1650 ℃, the relative density of the pre-sintered ceramic increases from 89.8% to 98.0%, and the average grain size of ceramics increases from 0.4 to 1.4 μm. Especially when the pre-sintering temperature exceeds 1550 ℃, the grains grow rapidly. The relative density of HIP post-treated Ce,Y:$SrHfO_3$ ceramics first increases and then decreases, because the higher pre-sintering temperature leads to the larger grain size, which means lower driving force of grain boundary migration in HIP post-treatment. Meanwhile high pre-sintering temperature produces intracrystalline pores, which can hardly be eliminated in HIP treatment.

Fig. 3(a) shows the photograph of the Ce,Y:$SrHfO_3$ ceramics vacuum-sintered at different temperatures for 2 h combined with the HIP post-treatment at 1800 ℃ for 3 h. The Ce,Y:$SrHfO_3$ ceramics pre-sintered at 1450 ℃ is still opaque after HIP post-treatment due to the insufficient densification and connected pores, which cannot be compressed with the aid of pressure. The Ce,Y:$SrHfO_3$ ceramics pre-sintered at 1600 and 1650 ℃ are also opaque after HIP post-treatment possibly due to the low driving force caused by large grain size and the remainning intracrystalline pores in the ceramics. After the HIP post-treatment, Ce,Y:$SrHfO_3$ pre-sintered at temperatures

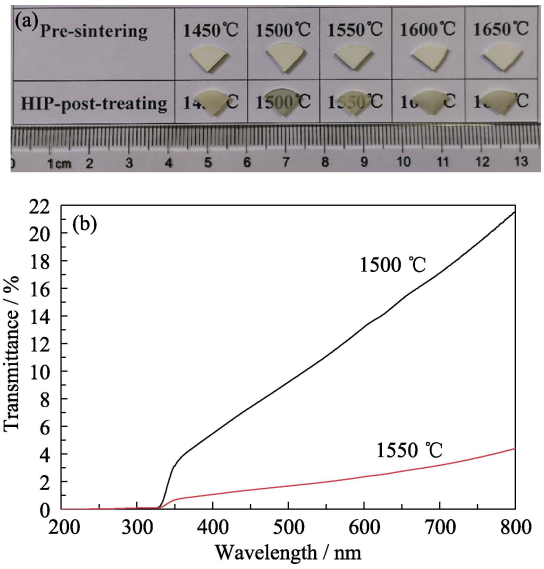

Fig. 3　(a) Photograph of the Ce,Y:$SrHfO_3$ ceramics vacuum-sintered at different temperatures combined with the HIP post-treatment and (b) in-line transmittance of the HIP post-treated Ce,Y:$SrHfO_3$ ceramics (1 mm thickness) pre-sintered at 1500 and 1550 ℃, respectively

within 1500 and 1550 ℃ become transparent and the text below the ceramics is legible. It indicates that the pre-sintering temperature has an important influence on the transparency of the ceramic. The in-line transmittance curves of the HIP post-treated Ce,Y:$SrHfO_3$ ceramics pre-sintered at 1500 and 1550 ℃ are shown in Fig. 3(b), and the former has the highest transmittance of 22% at 800 nm. Scintillation materials used in most fields like high energy physics and nuclear medicine equipment must be transparent, otherwise the visible light transformed from high energy rays is supposed to be self-absorbed and cannot reach the detectors behind.

The microstructure of the ceramic with the best transmittance was also analyzed as shown in Fig. 4. The FESEM micrographs of thermally etched surfaces and fractured surfaces of the HIP post-treated Ce,Y:$SrHfO_3$ ceramics pre-sintered at 1500 ℃ show very tiny number of pores. Compared with pre-sintered Ce,Y:$SrHfO_3$ ceramics, the Ce,Y:$SrHfO_3$ ceramics after HIP treatment show higher density and larger average grain size of 3.4 μm, which is still far smaller than that of the ceramics prepared *via* long-time vacuum sintering. The effective elimination of pores and the retention of fine grains are the key points for the preparation of transparent Ce,Y:$SrHfO_3$ ceramics by HIP treatment.

The luminescence and scintillation property of the sample with the best transmittance were evaluated. Fig. 5(a) shows the XEL spectra (X-ray Excited Luminescence, XEL) of the HIP post-treated Ce,Y:$SrHfO_3$ ceramics pre-sintered at 1500 ℃ and BGO single crystal

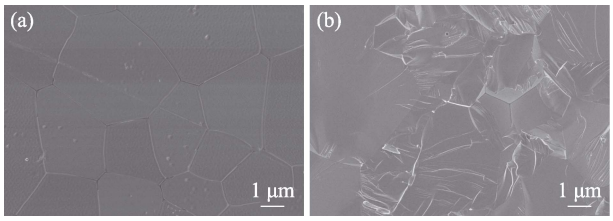

Fig. 4 FESEM micrographs of (a) thermally etched surfaces and (b) fractured surfaces of HIP post-treated Ce,Y:$SrHfO_3$ ceramics pre-sintered at 1500 ℃

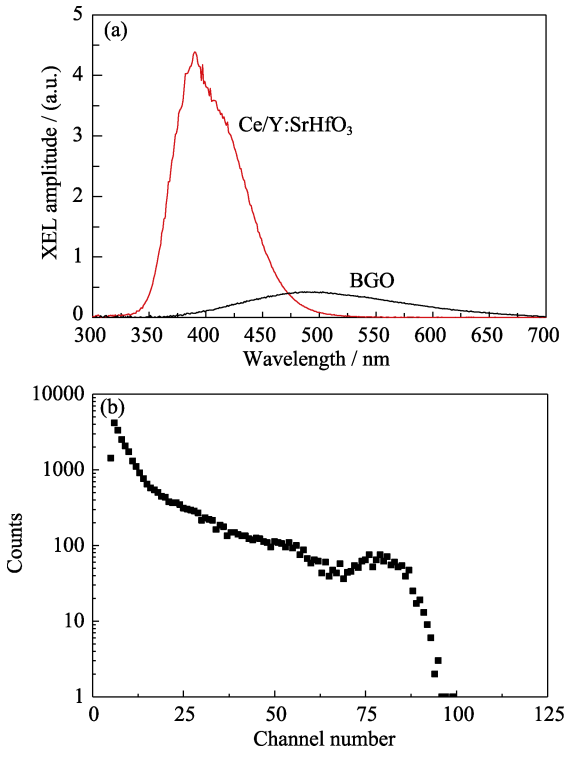

Fig. 5 (a) XEL spectra and (b) pulse height spectrum of the HIP post-treated Ce,Y:$SrHfO_3$ ceramics pre-sintered at 1550 ℃

at room temperature. The emission peak of Ce,Y:$SrHfO_3$ is situated at around 400 nm originating from the 5d-4f emission of Ce^{3+}. Comparing the integral of the emission spectra, the light output of Ce,Y:$SrHfO_3$ ceramics is 3.3 times higher than that of BGO commercial crystal. Fig. 5(b) shows the pulse height spectrum of the HIP post-treated Ce,Y:$SrHfO_3$ ceramics pre-sintered at 1500 ℃ under the 662 keV γ-ray excitation of ^{137}Cs source with 1 μs shaping time. Ce,Y:$SrHfO_3$ ceramics have a light yield of approximately 3700 ph/MeV which is less than half of that of BGO crystals. Comparison of overall scintillation efficiency derived from XEL spectra integrals and light yield measured in Ce,Y:$SrHfO_3$ ceramics and BGO crystal points to existing very slow components in the scintillation response of the former. The oxygen vacancies and related electron traps caused by reductive preparation atmosphere may be one of the reasons, and further study is needed for material optimization.

3 Conclusion

In this work, Ce,Y:$SrHfO_3$ powders were prepared by solid-state synthesis using the commercial HfO_2, $SrCO_3$, CeO_2, and Y_2O_3 as the starting materials. Pure $SrHfO_3$ phase is formed at 1200 ℃ for 8 h duration in air. Ce,Y:$SrHfO_3$ ceramics are successfully fabricated by (i) traditional long-time vacuum sintering and (ii) short-time vacuum pre- sintering combined with HIP post-treatment. The Ce,Y:$SrHfO_3$ ceramics sintered in vacuum at 1800 ℃ for 20 h are opaque due to the large grain size and residual pores. For the second preparation method, the average grain size of the pre-sintered Ce,Y:$SrHfO_3$ ceramics increases from 0.4 to 1.4 μm with the increase of pre-sintering temperature from 1450 to 1650 ℃. Subsequent HIP post-treatment successfully eliminates the pores, and the fine grain size is retained, both of which improve the optical quality of ceramics. The Ce,Y:$SrHfO_3$ ceramics pre-sintered at 1500 ℃ for 2 h with HIP post-treatment at 1800 ℃ for 3 h show the highest in-line transmittance of 22% at 800 nm. Overall scintillation efficiency derived from XEL spectra integral is 3.3 times higher than that of BGO crystals, while its light yield value is 3700 ph/MeV. The latter points to the presence of intense slow components in the scintillation response and requires further study.

References:

[1] NIKL M, YOSHIKAWA A. Recent R & D trends in inorganic single-crystal scintillator materials for radiation detection. *Advanced Optical Materials*, 2015, **3(4):** 463–481.

[2] NIKL M, MIHOKOVA E, PEJCHAL J, *et al*. Scintillator Materials—achievements, opportunities and puzzles. *IEEE Transactions on Nuclear Science*, 2008, **55(3):** 1035–1041.

[3] NIKL M. Scintillation detectors for X-rays. *Measurement Science and Technology*, 2006, **17:** R37–R54.

[4] NIKL M, LAGUTA V V, VEDDA A A. Complex oxide scintillators: material defects and scintillation performance. *Physica Status Solidi B-Basic Solid State Physics*, 2008, **245(9):** 1701–1722.

[5] MAO RI-HUA, ZHANG LI-YUAN, ZHU REN-YUAN. Optical and scintillation properties of inorganic scintillators in high energy physics. *IEEE Transactions on Nuclear Science*, 2008, **55(4):** 2425–2431.

[6] SEIICHI Y, NITTA H. Development of an event-by-event based radiation imaging detector using GGAG:Ce ceramic scintillator for X-ray CT. *Nuclear Instruments and Methods in Physics Research Section A: Accelerators, Spectrometers, Detectors and Associated Equipment*, 2018, **900:** 25–31.

[7] LIU SHU-PING, MARES J A, FENG XI-QI, *et al*. Towards bright and fast $Lu_3Al_5O_{12}$:Ce,Mg optical ceramics scintillators. *Advanced Optical Materials*, 2016, **4(5):** 731–739.

[8] YANAGIDA T, FUKABORI A, FUJIMOTO Y, A. *et al*. Scintillation properties of transparent $Lu_3Al_5O_{12}$ (LuAG) ceramics doped with different concentrations of Pr^{3+}. *Physica Status Solidi A-Applications and Materials Science*, 2011, **8(1):** 140–143.

[9] JI Y M, JIANG D Y, CHEN J J, *et al*. Preparation, luminescence and sintering properties of Ce-doped $BaHfO_3$ phosphors. *Optical Materials*, 2006, **28(4):** 436–440.

[10] SEFERIS I E, FIACZYK K, SPASSKY D, *et al*. Synthesis and luminescence properties of $BaHfO_3$:Pr ceramics. *Journal of Luminescence*, 2016, **189:** 148–152.

[11] JI YA-MING, JIANG DAN-YU, SHI JIAN-LIN. $La_2Hf_2O_7$:Ti^{4+} ceramic scintillator for X-ray imaging. *Journal of Materials Research*, 2005, **20(3):** 567–570.

[12] WAHID K, POKHREL M, MAO Y B. Structural, photoluminescence and radioluminescence properties of Eu^{3+} doped $La_2Hf_2O_7$ nanoparticles. *Journal of Solid State Chemistry*, 2016, **245:** 89–97.

[13] YI HAI-LAN, ZOU XIAO-QING, YANG YAN, *et al*. Fabrication of highly transmitting $LaGdHf_2O_7$ ceramics. *Journal of the American Ceramic Society*, 2011, **94(12):** 4120–4122.

[14] WANG ZHENG-JUAN, ZHOU GUO-HONG, ZHANG JIAN, *et al*. Luminescence properties of Eu^{3+}-doped lanthanum gadolinium hafnates transparent ceramics. *Optical Materials*, 2016, **71:** 5–8.

[15] AN L Q, ITO A, GOTO T. Fabrication of transparent $Lu_2Hf_2O_7$ by reactive spark plasma sintering. *Optical Materials*, 2013, **35(4):** 817–819.

[16] ZHOU GUO-HONG, WANG ZHENG-JUAN, ZHOU BO-ZHU, *et al*. Fabrication of transparent $Y_2Hf_2O_7$ ceramics *via* vacuum sintering. *Optical Materials*, 2013, **35(4):** 774–777.

[17] HAVLAK L, BOHACEK P, NIKL M, *et al*. Preparation and luminescence of $Lu_4Hf_3O_{12}$ powder samples doped by trivalent Eu, Tb, Ce, Pr, Bi ions. *Optical Materials*, 2010, **32(10):** 1372–1374.

[18] JOANNA J P, ZYCH E. Microwave-assisted hydrothermal synthesis and spectroscopic characteristics of $Lu_4Hf_3O_{12}$:Pr scintillator. *RSC Advances*, 2016, **6(61):** 56101–56107.

[19] BOHÁCEK P, TRUNDA B, BEITLEROVÁ A, *et al*. Rare-earth-free luminescent non-stoichiometric phases formed in SrO-HfO_2 ternary compositions. *Journal of Alloys and Compounds*, 2013, **580:** 468–474.

[20] JARÝ V, BOHÁČEK P, PEJCHAL J, *et al*. Scintillating ceramics based on non-stoichiometric strontium hafnate. *Optical Materials*, 2018, **77:** 246–252.

[21] JI Y M, JIANG D Y, QIN L S, *et al*. Preparation and luminescent properties of nanocrystals of Ce^{3+} activated $SrHfO_3$. *Journal of Crystal Growth*, 2005, **280(1/2):** 93–98.

[22] LOEF E V V, HIGGINS W M, GLODO J, *et al*. Scintillation properties of $SrHfO_3$:Ce^{3+} and $BaHfO_3$:Ce^{3+} ceramics. *IEEE Transactions on Nuclear Science*, 2007, **54(3):** 741–743.

[23] KUROSAWA S, PEJCHAL J, WAKAHARA S, *et al*. Optical properties and radiation response of Ce:$SrHfO_3$ prepared by the spark plasma sintering method. *Radiation Measurements*, 2013, **56:** 155–158.

[24] MIHÓKOVÁ E, JARÝ V, FASOLI M, *et al*. Delayed recombination and excited state ionization of the Ce^{3+} activator in the $SrHfO_3$ host. *Chemical Physics Letters*, 2013, **7(3):** 228–231.

[25] CHIBA H, KUROSAWA S, HARATA K, *et al*. Luminescence properties of the Mg co-doped Ce:$SrHfO_3$ ceramics prepared by the spark plasma sintering method. *Radiation Measurements*, 2016, **90:** 287–291.

[26] KAMADA K, KUROSAWA S, SHOJI Y, *et al*. Luminescence and scintillation properties of Ce doped $SrHfO_3$ based eutectics. *Optical Materials*, 2015, **41:** 41–44.

[27] LING JUN-RONG, ZHOU YOU-FU, XU WEN-TAO, *et al*. Red-emitting YAG:Ce,Mn transparent ceramics for warm WLEDs application. *Journal of Advanced Ceramics*, 2020, **9(1):** 45–54.

[28] LI XIAO-YING, LIU QIANG, HU ZE-WANG, *et al*. Influence of ammonium hydrogen carbonate to metal ions molar ratio on co-precipitated nanopowders for TGG transparent ceramics. *Journal of Inorganic Materials*, 2019, **34(7):** 791–796.

[29] MOHAMMADI F, MIRZAEE O, TAJALLY M, *et al*. The effects of ball milling time on the rheological, optical, and microstructural properties of YAG transparent ceramics. *International Journal of Applied Ceramic Technology*, 2020, **17(3):** 1119–1127.

[30] ZHANG LEI, YANG JUN, YU HONG-YU, *et al*. High performance of La-doped Y_2O_3 transparent ceramics. *Journal of Advanced Ceramics*, 2020, **9(4):** 493–502.

[31] LOEF E V V, WANG Y M, MILLER S R, *et al*. Effect of microstructure on the radioluminescence and transparency of Ce-doped strontium hafnate ceramics. *Optical Materials*, 2010, **33(1):** 84–90.

[32] KENNEDY B J, HOWARD C J, CHAKOUMAKOS B C. High-temperature phase transitions in $SrHfO_3$. *Physical Review B*, 1999, **60:** 2972–2975.

[33] LOUREIRO S M, GAO Y, VENKATARAMANI V. Stability of Ce(III) activator and codopant effect in $MHfO_3$ (M=Ba, Sr) scintillators by XANES. *Journal of the American Ceramic Society*, 2005, **88(1):** 219–221.

[34] LIU ZI-YU, TOCI G, PIRRI A, *et al*. Fabrication, microstructures, and optical properties of Yb:Lu_2O_3 laser ceramics from co-precipitated nano-powders. *Journal of Advanced Ceramics*, 2020, **9(6):** 674–682.

[35] QIAN KANG, PAN YU-BAI, HU ZE-WANG, *et al*. Influence of co-doped alumina on the microstructure and radioluminescence of $SrHfO_3$:Ce ceramics. *Journal of the European Ceramic Society*, 2020, **40(2):** 449–455.

热等静压烧结制备细晶粒 Ce,Y:$SrHfO_3$ 闪烁陶瓷

朱丹阳[1,2], 钱 康[1,3], 陈肖朴[1,2], 胡泽望[1,2], 刘 欣[1,2], 李晓英[1,2], 潘裕柏[3], MIHÓKOVÁ Eva[4], NIKL Martin[4], 李 江[1,2]

(1. 中国科学院 上海硅酸盐研究所, 透明光功能无机材料重点实验室, 上海 201899; 2. 中国科学院大学 材料科学与光电工程中心, 北京 100049; 3. 上海师范大学 物理系, 上海 200234; 4. 捷克科学院 物理研究所, 捷克 布拉格 16200)

摘 要: Ce:$SrHfO_3$ 陶瓷因具有高密度和高有效原子序数, 对高能射线具有很强的阻止能力。同时, Ce:$SrHfO_3$ 陶瓷还具有快衰减和高能量分辨率等优异的闪烁性能, 引起了研究人员的广泛关注。由于传统的烧结方法难以实现非立方结构 Ce:$SrHfO_3$ 陶瓷的透明化, 本研究采用真空长时烧结和短时真空预烧结合热等静压烧结(Hot Isostatic Pressing, HIP)方法制备 Ce,Y:$SrHfO_3$ 陶瓷。以金属氧化物和碳酸盐为原料, 1200 ℃下煅烧 8 h 可以获得平均粒径为 152 nm 的纯相 Ce,Y:$SrHfO_3$ 粉体。1800 ℃真空烧结 20 h 获得平均晶粒尺寸为 28.6 μm 的不透明的 Ce,Y:$SrHfO_3$ 陶瓷, 而两步烧结法可以制备光学透过率良好的 Ce,Y:$SrHfO_3$ 陶瓷。本研究详细分析了陶瓷致密化过程中微结构的演变, 探究了预烧结温度对 Ce,Y:$SrHfO_3$ 陶瓷密度、显微结构和光学透过率的影响。真空预烧(1500 ℃×2 h)结合 HIP 后处理(1800 ℃×3 h, 200 MPa Ar)所获得的 Ce,Y:$SrHfO_3$ 陶瓷在 800 nm 处的最高直线透过率为 21.6%, 平均晶粒尺寸仅为 3.4 μm。在 X 射线激发下, Ce,Y:$SrHfO_3$ 陶瓷在 400 nm 处产生 Ce^{3+} 5d-4f 发射峰, 其 XEL 积分强度比商用锗酸铋(BGO)晶体高 3.3 倍, Ce,Y:$SrHfO_3$ 陶瓷在 1 μs 门宽下的光产额约为 3700 ph/MeV。良好的光学和闪烁性能可以拓宽 Ce,Y:$SrHfO_3$ 陶瓷在闪烁探测领域的应用。

关 键 词: Ce,Y:$SrHfO_3$ 陶瓷; 热等静压烧结; 微观结构; 晶粒细化; 闪烁性能

中图分类号: TQ174 **文献标志码**: A